Supplementary Information (SI) for Environmental Science: Nano.

A synergistic co-catalyst $FeMoO_4$@Fe_7S_8 based on strong interactions/complexation between Fe-Mo and C_n-N(O) for smartphone-based visually colorimetric assay of tetracyclines

Jingjing Gu[1,2], Hailong Gong[1], Yuhao Li[1], Qinqin Ma[1], Xiaofeng Hou[1], Siyu Shen[1], Tingting Liu[1,3*], Xuedong Wang[2*]

[1]School of Environmental Science and Engineering, Suzhou University of Science and Technology, Suzhou, 215009, China

[2]College of Public Health and Management, Wenzhou Medical University, Wenzhou 325035, China

[3]Jiangsu Key Laboratory of Environmental Science and Engineering, Suzhou University of Science and Technology, Suzhou 215009, China

* Corresponding author: Tingting Liu, Email: liutt@mail.usts.edu.cn; Xuedong Wang, Email: zjuwxd@163.com

Tel: 86-512-68095950; Fax: 86-512-68095950

Main contents

Text S1. Synthesis of $FeMoO_4$ nanoparticles, Fe_7S_8 nanosheet, and $FeMoO_4$@Fe_7S_8-X NPs

1.1. Synthesis of $FeMoO_4$ nanoparticles

Firstly, 3 mM of $NaMoO_4 \cdot 2H_2O$ was dissolved in 30 mL ultra-pure water for sample A. Similarly, 5 mM $FeCl_3 \cdot 6H_2O$ and 10 mM NaAc were added to 30 mL ultra-pure water, which was marked as sample B. Then, the solution A and B were mixed for stirring 1 h and moved to autoclave. The ensuing reaction occurs at 200 °C for 24 h. The as-obtained $FeMoO_4$ nanoparticles ($FeMoO_4$ NPs) were washed three times with ultra-pure water and ET and finally dried in a vacuum drying oven at 60 °C for 4 h.

1.2. Synthesis of Fe_7S_8 nanosheets

2.73 mM $FeCl_2 \cdot 4H_2O$ and 3.6 mM TH were dissolved to 100 mL EG and stirred into the well-distributed solution. Then, the resulting mixture was put into the autoclave and heated to 200 °C for 12 h. The step of washing and drying method was the same as above, and the as-obtained Fe_7S_8 nanosheets.

1.3 Synthesis of $FeMoO_4$@Fe_7S_8-X NPs

The $FeCl_3 \cdot 6H_2O$, $Na_2MoO_4 \cdot 2H_2O$, and TH were used as Fe, Mo and S sources, respectively, to prepare three aforementioned nanomaterials. The $FeMoO_4$@Fe_7S_8-X NPs were successfully fabricated by a facile hydrothermal approach. Briefly, 3 mM $Na_2MoO_4 \cdot 2H_2O$, 4 mM OA, and 15 mM TH were dissolved in 40 mL ultra-pure water, which is denoted as sample A. Meanwhile, 5 mM $FeCl_3 \cdot 6H_2O$ and 10 mM NaAc were added to 20 mL EG, stirring to form an orange-red mixture solution (sample B). Next, the as-prepared sample B was mixed with sample A and stirred for ~1 h. The mixed solution was poured into an autoclave at 200 ℃ for 24 h. The as-obtained $FeMoO_4$@Fe_7S_8-1 NPs were collected by centrifugation, washing three times with ultra-pure water and ET, respectively, and dried at 60 °C for 4 h in a vacuum oven. Besides, other three kinds of nanomaterials were prepared with different ratios of Fe and NaAc at 1:4, 1:5 and 1:6 by the above-mentioned method.

Text S2. Materials and reagents

A series of analytical or chromatographic-grade chemicals and reagents were purchased and used in the following experiments. NaAc (99.0%) and *p*-benzoquinone (PBQ, 99.2%) were acquired from Aladdin. Hydrogen peroxide (H_2O_2, 30.0 %), hydrated copper sulfate ($CuSO_4 \cdot 5H_2O$, 99.0%), aluminum nitrate nonahydrate ($Al(NO_3)_3 \cdot 9H_2O$, 99.0%), zinc sulfate heptahydrate ($ZnSO_4 \cdot 7H_2O$,

99.0%), cobalt (II) nitrate hexahydrate ($Co(NO_3)_2 \cdot 6H_2O$, 99.0 %), silver nitrate ($AgNO_3$, 99.8%) were obtained from Adams. The following reagents were procured from Tansoole, including acetic acid glacial (HAc, 99.5%), dimethyl sulfoxide (DMSO, 99.5%), ethylene glycol (EG, 99.5%), ethanol (ET 99.0%), iron(III) chloride hexahydrate ($FeCl_3 \cdot 6H_2O$, 99.0%), sodium molybdate dihydrate ($Na_2MoO_4 \cdot 2H_2O$, 99.0%), thiourea (TH, 99.0%), 3,3',5,5'-tetramethylbenzidine (TMB, 99.0%), *o*-phenyl-enediamine (OPD, 99.0%), 2,2'-azino-bis(3-ethylbenzothiazoline-6-sulfonic acid) (ABTS, 97.0%), 3,3'-diaminobenzidine tetrahydrochloride (DAB, 98.0%), dihydroethidium (HE, 98.0%), terephthalic acid (TA, 98.0%), ethylenediaminetetraacetic acid (EDTA, 99.0%), citric acid (CA, 98.0%), nitrilotriacetic acid (NTA, 99.0%), oxalic acid (OA, 99.0%), tetracycline (TC, 98.0%), oxytetracycline (OTC, 98.0%), doxycycline hydrochloride (DOX, 98.0%), chlortetracycline (CTE, 98.0%), midecamycin (MID, 98.0%), erythromycin (ERY, 98.0%), sulfathiazole (STZ, 98.0%), sulfamethoxazole (SMZ, 98.0%), sulfamethoxazole (SDM, 98.0%), and cefotaxime (CTX, 98.0%). The standard solutions of Ni^{2+}, Hg^{2+}, Pb^{2+}, Se^{4+}, As^{3+}, NO_2^-, and PO_4^{2-} were provided by the China Institute of Metrology (Beijing, China). Iron chloride tetrahydrate ($FeCl_2 \cdot 4H_2O$, 98.0%), 5,5-dimethyl-1-pyrroline N-oxide (DMPO, 97.0%), sodium oxalate (Ox, 99.5%), and 2',7'-dichlorodihydrofluorescein (DCFH, 98.0%) were supplied by Macklin. All reagents were used directly without further purification, and ultra-pure water ((>18.2 MΩ) was fabricated from a Milli-Q membrane-purification system (Bedford, MA, USA). All milk samples were purchased from local supermarkets in Suzhou.

Text S3. Instruments

The following instruments were used to obtain the spectral information of as-prepared nanomaterials and analyze the concentrations of TCs: LC-20AT Shimadzu HPLC equipped with a diode-array detector (HPLC-DAD, Tokyo, Japan) and FS-5 fluorescence spectrometer (Edinburgh, UK). Several equipments were employed to characterize the morophologies and physicochemical properties of $FeMoO_4$ nanoparticles and Fe_7S_8 nanosheets, and $FeMoO_4$@Fe_7S_8-X NPs: scanning electron microscope (SEM, Quanta FEG 250, USA), high-resolution transmission electron microscope (HRTEM, FEI Tecnai F20, USA), X-ray diffractometer (XRD, Bruker D8 advance, Germany), UV-Vis spectrophotometer (UV-Vis, UV-5500PC, China), automatic surface area and porosity analyzer (TriStar II Plus 3030, USA), hysteresis loop test (VSM, LakeShore7404, USA), X-ray photoelectron spectrometer (XPS, Thermo Scientific ESCALAB 250Xi, USA), electron

paramagnetic resonance spectrometer (EPR, Bruker EMXplus-6, Germany), and Fourier transform infrared spectrometer (FTIR, Nicolet iS50, USA)

Text S4. Optimization of the experimental conditions

Some important reaction parameters were optimized to investigate their influences on the catalytic performance of $FeMoO_4$@Fe_7S_8-1 NPs. These parameters included buffer type (HAc-NaAc, Tris- HCl, and PBS), buffer pH (3.2-6.0), incubation temperature (20-55 ℃), incubation time (0-35 min), $FeMoO_4$@Fe_7S_8-1 NPs concentration (5-50 μg mL^{-1}), different chromogenic substrates (ABTS, DAB, TMB, OPD, and Strach-Nal), and type of $FeMoO_4$@Fe_7S_8-X NPs ($FeMoO_4$@Fe_7S_8-1 NPs, $FeMoO_4$@Fe_7S_8-2 NPs, $FeMoO_4$@Fe_7S_8-3 NPs, and $FeMoO_4$@Fe_7S_8-4 NPs). A total of 75 μL $FeMoO_4$@Fe_7S_8-X NPs (20 μg mL^{-1}), 100 μL of TMB (6 mM), 75 μL of H_2O_2 (50 mM) were introduced into 1650 μL of HAc-NaAc buffer (0.2 M, pH 3.6). Using external magnets to separate the $FeMoO_4$@Fe_7S_8-1 NPs. The absorbance value at 654 nm (A_{654}) was measured after incubation.

Text S5. The peroxidase-like (POD) activity of $FeMoO_4$@Fe_7S_8-1 NPs

The POD activity of $FeMoO_4$@Fe_7S_8-1 NPs was examined by means of a series of colorimetric assay in the presence of H_2O_2 and TMB. The experiments were carried out in five systems: $FeMoO_4$@Fe_7S_8-1 NPs+TMB+H_2O_2, TMB+H_2O_2, $FeMoO_4$@Fe_7S_8-1 NPs+TMB, $FeMoO_4$@Fe_7S_8-1 NPs+H_2O_2, and TMB. The $FeMoO_4$@Fe_7S_8-1 NPs (75 μL, 20 μg mL^{-1}), TMB (100 μL, 6mM), and H_2O_2 (75 μL, 50 mM) were added to HAc-NaAc buffer (1650 μL, 0.2 M, pH=3.6) and then incubated at 40 ℃ for 20 min. Using external magnets to separate the $FeMoO_4$@Fe_7S_8-1 NPs. Then, the solution was detected in the wavelength range of 400-750 nm by a UV-Vis spectrophotometer. Also, the POD activity was verified by the characteristic color of other chromogenic substrates, such as ABTS, DAB, and OPD.

The cyclic voltammetry (CV) and electrochemical impedance spectroscopy (EIS) tests were performed using a Chenhua CHI660D workstation with $FeMoO_4$@Fe_7S_8-1 NPs, $FeMoO_4$ nanoparticles or Fe_7S_8 nanosheets as the working electrode, saturated KCl solution as the counter electrode, and Ag/AgCl as the reference electrode, respectively.

Text S6. Steady-state kinetics of the $FeMoO_4$@Fe_7S_8-1 NPs

To systematically evaluate the POD activity of $FeMoO_4$@Fe_7S_8-1 NPs, the steady-state kinetics of this nanocomposite was probed under the following conditions: incubation temperature, 40 ℃; a constant H_2O_2 concentration, 2 mM; and varying TMB concentrations (0.2-6.0 mM) in the mixed

system of HAc-NaAc+$FeMoO_4$@Fe_7S_8-1 NPs. Also, the catalytic kinetics was also investigated at a constant TMB concentration (6 mM) and varying H_2O_2 concentrations (0.2-6.0 mM), while remaining other same reaction conditions. Subsequently, the kinetics parameters of the POD activity were computed on the basis of Michaelis-Menten equation:

$$v_0 = \frac{V_{max}[S]}{K_m + [S]}$$

where v_0 is the initial reaction rate, V_{max} is the maximum reaction rate, K_m is the Michaelis-Menten constant (the substrate concentration at half the maximum reaction rate), and $[S]$ is the TMB concentration.

Text S7. Selectivity, anti-interference and stability of the colorimetric sensor

To investigate the selectivity of the above standard mixed system towards TCs, a wide range of interfering substances were fortified, including cations (Ag^+, Pb^{2+}, Al^{3+}, As^{3+}, Co^{2+}, Se^{4+}, Mg^{2+}, K^+, Zn^{2+}, Ni^{2+}, Hg^{2+}, Cu^{2+}, Mn^{2+}, Na^+, and Ca^{2+}), anions (NO_2^-, PO_4^{2-}, and Cl^-), biological micromolecules (L-Threonine, L-Alanine, L-Serine, L-Histidine, L-Leucine, L-Tryptophan, D-Methionine, L-Glutamicacid, L-Malicacid, Glu, Cys, AA, and UA) and other antibiotics (MID, ERY, STZ, SMZ, SDM, and CTX). The concentrations of TCs, including TC, OTC, DOX, and CTC, were all set at 20 μM. In contrast, the concentrations of other interfering substances were all at 200 μM, i.e., 10-fold as high as those of TCs.

To ensure the stability of as-constructed colorimetric sensor for TCs, the post-reaction $FeMoO_4$@Fe_7S_8-1 NPs were collected by centrifugation. The above experimental procedures were repeated after washing and drying, and the corresponding A_{654} value was measured to evaluate changes in absorbance intensity during recycling use.

Text S8. Pretreatment procedures for the real-world water and milk samples

To evaluate the feasibility of the $FeMoO_4$@Fe_7S_8-1 NPs based colorimetric assay, the 4 of real-world water and 11 of milk samples were collected and used for detecting OTC, including aquaculture waters from fish-shrimp-crab mixed pond, fish pond, shrimp pond, and crab pond, as well as various milk, including pure milk (whole milk, low-fat milk, and defatted milk), fresh milk (whole milk, low-fat milk, and defatted milk), buffalo milk and goat milk. Prior to analysis, water samples were filtered using 0.22-μm cellulose filter membranes. By way of contrast, acetonitrile (2 mL) was added to 1 mL of milk sample for the purpose of removing proteins. After filtration and

centrifugation, the supernatant was collected, and the subsequent procedures were similar as described above.

Text S9. The detailed measurement of smartphone-based sensing analysis

Different concentration of OTC standard solutions (0, 1, 4, 7, 10, 13, 16,19,20 μM) were added into the "$FeMoO_4$@Fe_7S_8-1 NPs+TMB+H_2O_2" system, and incubated for 20 min at 40 ℃. Firstly, the reaction solutions were sequentially transferred to 96-well plates, and placed into our auxiliary imaging interferogram device to capture images of the color changes by using a smartphone immediately. Then, the captured image was imported to "Thing identity" APP for established the standard curve of OTC. The method for detecting actual samples was operated as described above. According to the established standard curve, the relevant image of actual sample was used to analyze the concentration based on our APP (the detailed operations was seen in Fig. S3).

Text S10. HPLC-DAD detection for OTC

The concentration of OTC was determined by HPLC-DAD analysis in real-world water and milk samples. The HPLC-DAD instrument (Shimadzu HPLC, LC-20AT, Japan) was equipped with an Venusil XBP C_{18} column (4.6×250 mm, 5 μm) and a diode-array detector operated at a wavelength of 355 nm. The mobile phase consisted of 0.1% formic acid and acetonitrile (v:v=80%:20%) at a flow rate of 1.0 mL/min. The sample injection volume was 10 μL. The linear relationship between peak area and concentration of OTC is presented in Fig. S4.

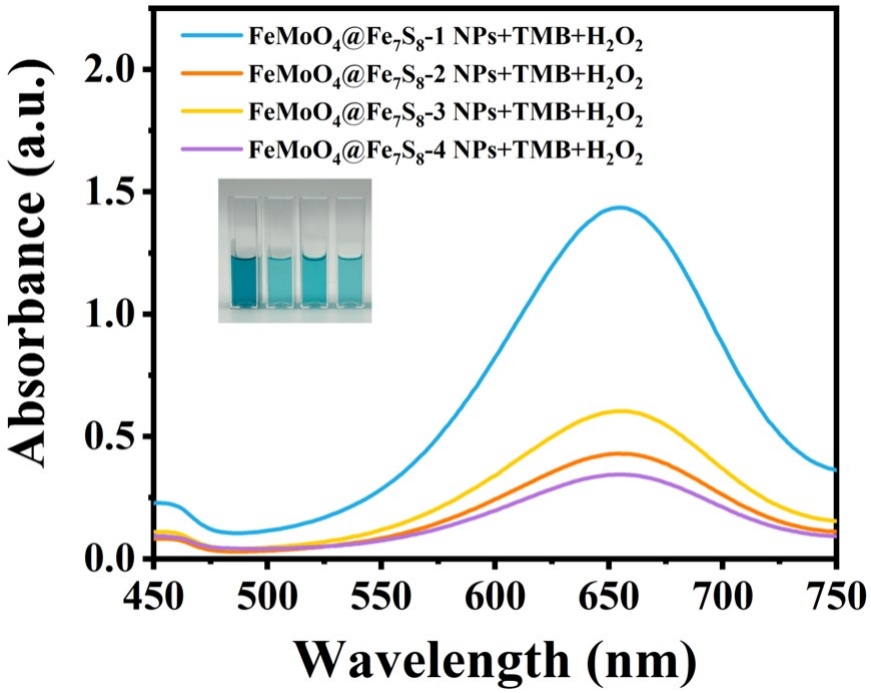

Fig. S1. UV-Vis spectra in the $FeMoO_4$@Fe_7S_8-X NPs (1, 2, 3, 4) +TMB+H_2O_2 systems.

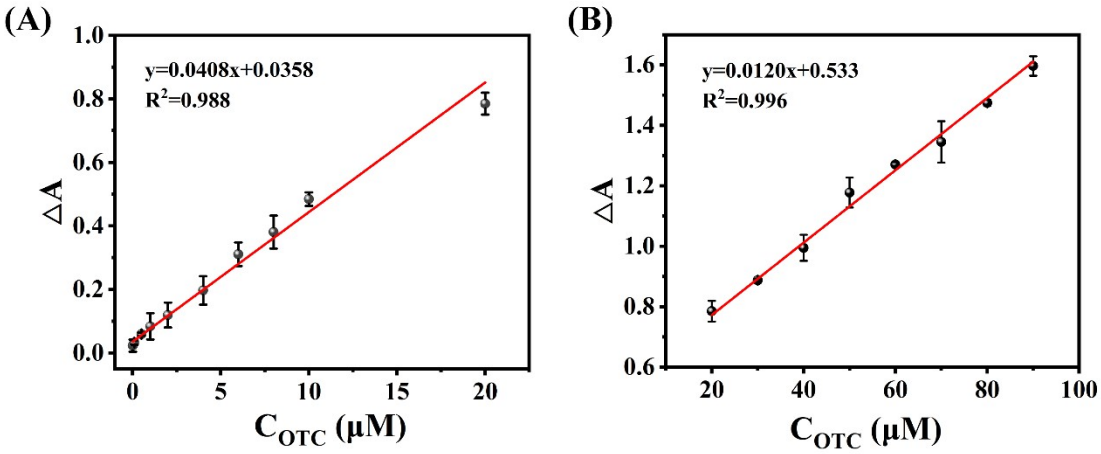

Fig. S2. (A-B) Linear plots of OTC in the range of 0.1-90 μM. The error bars represent the standard deviation (*n*=3).

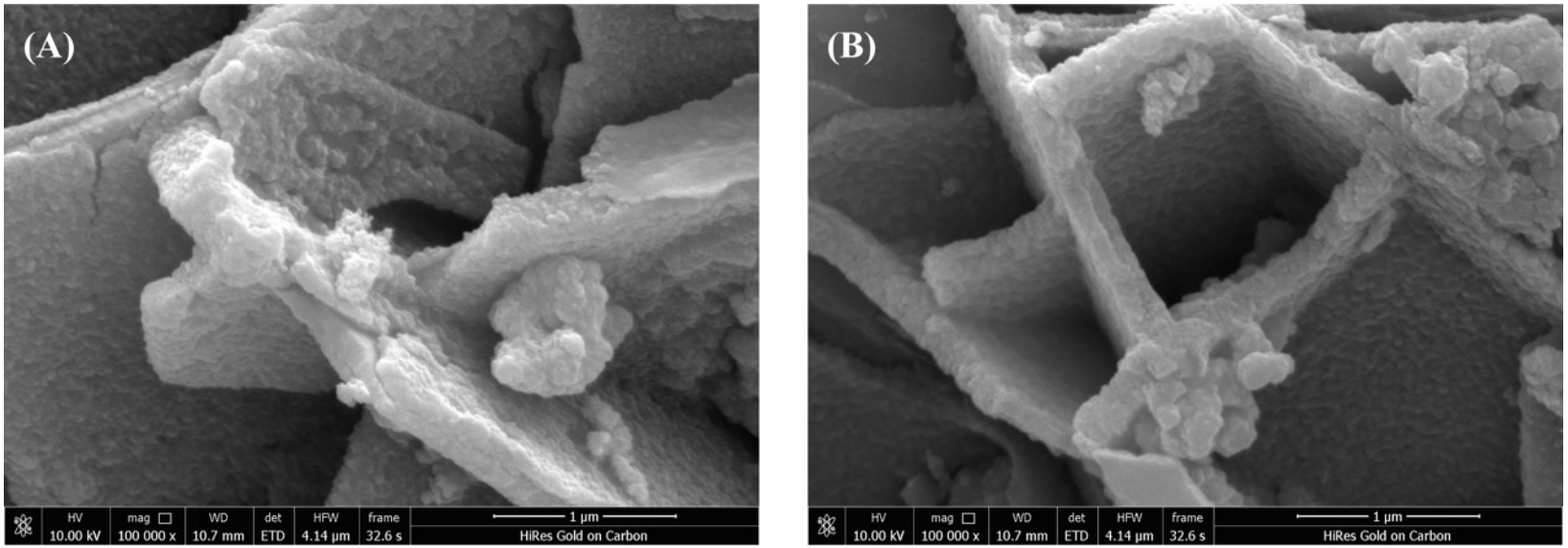

Fig. S3. (A) SEM image of $FeMoO_4$@Fe_7S_8-1 NPs; (B) SEM image of $FeMoO_4$@Fe_7S_8-1 NPs after 7 months of storage.

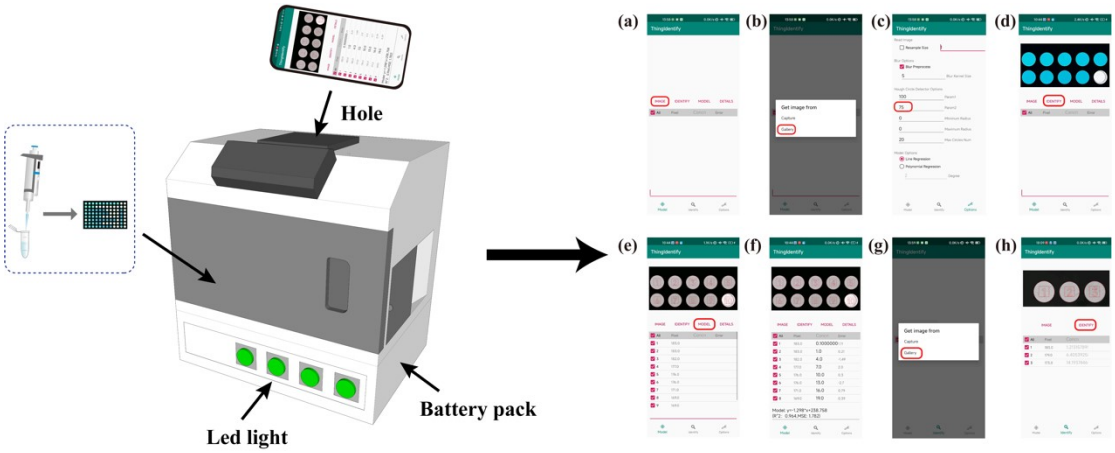

Fig. S4. Schematic illustration on the smartphone-based colorimetric assay platform.

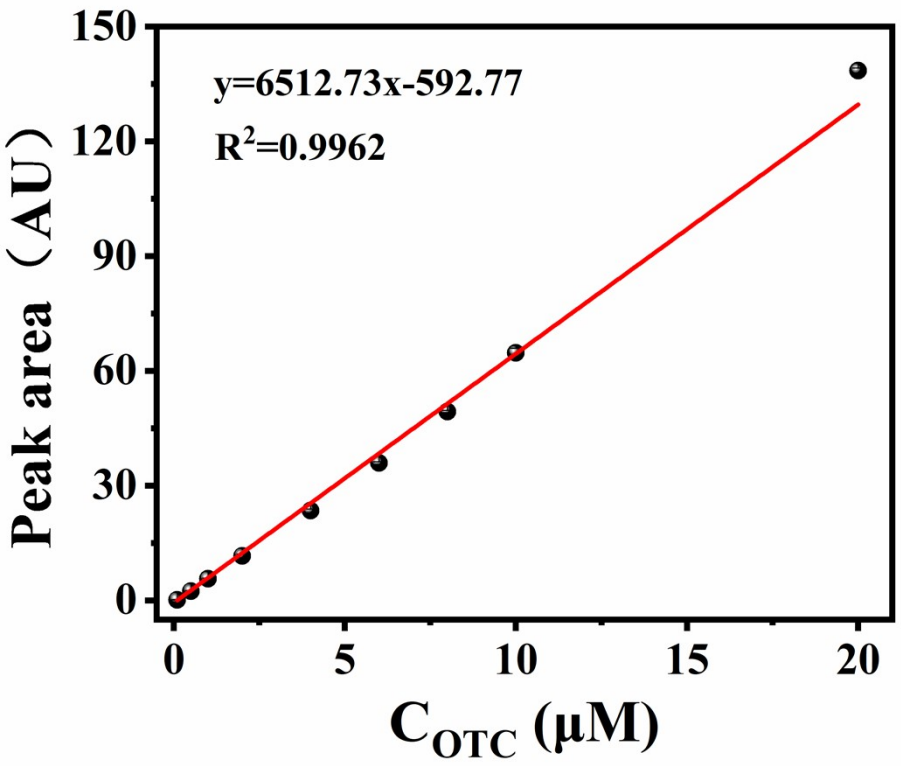

Fig. S5. Linear relationship between peak area and concentration of OTC (0.1-20 μM)

Table S1. BET testing data.

Samples	Surface area (m^2/g)	Pore volume (cm^3/g)	Pore size (nm)
Fe_7S_8	13.46	0.058	20.36
$FeMoO_4$	2.18	0.0094	24.78
$FeMoO_4$@Fe_7S_8-1 NPs	6.31	0.024	18.12

Table S2. Comparison of the kinetics parameters of $FeMoO_4$@Fe_7S_8-1 NPs with other TMCs-based nanozymes

Nanozymes	K_m (mM)		V_{max} (10^{-8} M/s)		Refs.
	TMB	H_2O_2	TMB	H_2O_2	
Fe_3O_4	0.42	0.97	5.5	7.02	[1]
His-Fe_3O_4	0.42	0.54	6.72	7.02	
Fe_3O_4@SiO_2@$NiCo_2S_4$	0.26	0.05	3.33	5.12	[2]
Fe/NC	0.13	7.37	4.07	6.41	[3]
Fe_7S_8-100	0.13	0.29	17.02	14.52	[4]
Fe_2MoO_4	3.06	0.26	1.81	8.22	[5]
MoS_2	5.23	0.48	1.44	0.21	[6]

SWCNTS@MoS_2	0.19	1.51	4.66	0.45	
$FeMoO_4$@Fe_7S_8-1 NPs	0.09	0.33	3.10	3.24	This work.

Reference

[1] X. Yuan, S. Cheng, L. Chen, Z. Cheng, J. Liu, H. Zhang, J. Yang and Y. Li, Iron oxides based nanozyme sensor arrays for the detection of active substances in licorice, *Talanta*, 2023, **258**, 124407.

[2] X. Wang, M. Chen and L. Zhao, Development of a colorimetric sensing assay for ascorbic acid and sarcosine utilizing the dual-class enzyme activity of Fe_3O_4@SiO_2@$NiCo_2S_4$, *Chem. Eng. J.*, 2023, **468**, 143612.

[3] Y. Miao, M. Xia, C. Tao, J. Zhang, P. Ni, Y. Jiang and Y. Lu, Iron-doped carbon nitride with enhanced peroxidase-like activity for smartphone-based colorimetric assay of total antioxidant capacity, *Talanta*, 2024, **267**, 125141.

[4] Y. Ding, T. Liu, Q. Wang, J. Gu, Y. Li, Z. Zhang and X. Wang, An enrichment-colorimetry integration strategy for nM-level Hg^{2+} detection in environmental waters based on an efficient Fe_7S_8-100 nanozyme and smartphone-based visual assay, *Sensor Actuat B-Chem.*, 2023, **390**, 133995.

[5] Y. Fu, Z. Zhao, Y. Shi, K. Xu, J. Zhang, H. Niu and Y. Xu, Hybridization chain reaction-mediated Fe_2MoO_4 bimetallic nanozyme for colorimetric risk prediction of bladder cancer, *Biosens. Bioelectron.*, 2022, **210**, 114272.

[6] L. Feng, L. Zhang, S. Chu, S. Zhang, X. Chen, Y. Gong, Z. Du, G. Mao and H. Wang, One-pot fabrication of nanozyme with 2D/1D heterostructure by in-situ growing MoS_2 nanosheets onto single-walled carbon nanotubes with enhanced catalysis for colorimetric detection of glutathione, *Anal. Chim. Acta*, 2022, **1221**, 340083.